

Decoherence of fiber light sources using a single-trench fiber

Huahui Zhang(张华辉), Weili Zhang(张伟利), Zhao Wang(王昭), Hongyang Zhu(朱洪杨), Chao Yu(余超), Jiayu Guo(郭佳宇), Shanshan Wang(王珊珊), and Yunjiang Rao(饶云江)

Citation: Chin. Phys. B, 2020, 29 (**12**): 124210. DOI: 10.1088/1674-1056/abb6
Journal homepage: http://cpb.iphy.ac.cn; http://iopscience.iop.org/cpb

What follows is a list of articles you may be interested in

Two-dimensionally controllable DSR generation from dumbbell-shaped mode-locked all-fiber laser

Zhi-Yuan Dou(窦志远), Bin Zhang(张斌), Jun-Hao Cai(蔡君豪), Jing Hou(侯静)
Chin. Phys. B, 2020, 29 (**9**): 094201. DOI: 10.1088/1674-1056/ab9de1

High efficiency sub-nanosecond electro-optical *Q*-switched laser operating at kilohertz repetition frequency

Xin Zhao(赵鑫), Zheng Song(宋政), Yuan-Ji Li(李渊骥), Jin-Xia Feng(冯晋霞), Kuan-Shou Zhang(张宽收)
Chin. Phys. B, 2020, 29 (**8**): 084205. DOI: 10.1088/1674-1056/ab8ac4

Gain-induced large optical torque in optical twist settings

Genyan Li(李艮艳), Xiao Li(李肖), Lei Zhang(张磊), Jun Chen(陈君)
Chin. Phys. B, 2020, 29 (**8**): 084201. DOI: 10.1088/1674-1056/ab9616

Optical nonreciprocity in a piezo-optomechanical system

Yu-Ming Xiao(肖玉铭), Jun-Hao Liu(刘军浩), Qin Wu(吴琴), Ya-Fei Yu(於亚飞), Zhi-Ming Zhang(张智明)
Chin. Phys. B, 2020, 29 (**7**): 074204. DOI: 10.1088/1674-1056/ab8abf

A compact electro-absorption modulator based on graphene photonic crystal fiber

Guangwei Fu(付广伟), Ying Wang(王颖), Bilin Wang(王碧霖), Kaili Yang(杨凯丽), Xiaoyu Wang(王晓愚), Xinghu Fu(付兴虎), Wa Jin(金娃), Weihong Bi(毕卫红)
Chin. Phys. B, 2020, 29 (**3**): 034209. DOI: 10.1088/1674-1056/ab6838

Decoherence of fiber light sources using a single-trench fiber*

Huahui Zhang(张华辉)[1], Weili Zhang(张伟利)[1,†], Zhao Wang(王昭)[1], Hongyang Zhu(朱洪杨)[1], Chao Yu(余超)[2], Jiayu Guo(郭佳宇)[1], Shanshan Wang(王珊珊)[1], and Yunjiang Rao(饶云江)[1]

[1] *School of Information and Communication Engineering, University of Electronic Science and Technology of China, Chengdu* 611731, *China*
[2] *China Second Institute of Railway Engineering Group Co. LTD, Chengdu* 610031, *China*

(Received 9 May 2020; revised manuscript received 6 August 2020; accepted manuscript online 9 September 2020)

Decoherence of fiber laser sources is of great importance in imaging applications, and most current studies use ordinary multi-mode fibers (MMFs). Here, a newly designed single-trench fiber (STF) is investigated to reduce the spatial coherence of fiber light source and compared with MMFs. By bending two fibers with different turns, speckle contrast of a 0.8-m-long STF can be reduced from 0.13 to 0.08, while a 0.8-m-long MMF shows an inverse result. Through speckle contrast and decoupling-mode analysis, the reason of this inverse trend is revealed. Firstly, the STF supports more modes than the MMF due to its larger core diameter. Secondly, mode leak from the first core of the STF can couple to the second core when bending the STF. Thus, power distribution among high and low-order modes become more even, reducing the spatial coherence considerably. However, in the MMF, high-order modes become leaky modes and decrease slightly when bending the fiber. This work provides a new method to modulate coherence of light source and a new angle to study decoherence principle using special fibers.

Keywords: single-trench fiber, multi-mode fiber, bending fiber, speckle contrast

PACS: 42.81.–i, 42.87.–d **DOI:** 10.1088/1674-1056/abb65f

1. Introduction

The mutual interference of light source can generate speckle, which extensively occurs in optical systems.[1] Performance of imaging systems illuminated with spatial coherent light sources would be deteriorated by speckles, so it is imperative to suppress speckles in these applications, such as laser radar,[2] digital holography,[3,4] laser inherent field imaging,[5] speckle-free full-field imaging[6] and optical coherence tomography (OCT).[7–9] Researchers have come up with practical methods to cope with this problem.[10–13] The typical methods for suppressing speckle include temporal averaging with a moving diffuser, polarization diversity, wavelength/angle diversity, temporal and spatial modulation.[14,15] The aforementioned methods can achieve a partially coherent or fully incoherent light. Apart from these methods, exploiting MMFs to reduce speckles is also known as an effective approach, due to its characteristics such as excellent directionality as well as being compatible with fiber systems/devices.

It is known that spatial coherence can be reduced with excitation of more spatial modes.[16,17] Therefore, a large-mode area step-index MMF, which supports a large number of transverse/spatial modes, can be used to restrain speckle formation.[18,19] Another key factor is to make the excited spatial modes decoherent. The principle of decoherence in MMFs is that with accumulation of dispersion, intermodal delay can surpass the coherence length of light source. Usually, this method requires a relatively long length of fiber to realize low coherence.[20] For a fixed MMF structure, to get sufficient low spatial coherence, apart from increasing the power of light source,[21] one should excite more effective spatial eigenmodes of the MMF. This could be achieved by bending the MMF used or off-set splicing of the initial light injection. However, ordinary MMFs are poorly suitable to excite high-order modes through bending, since the modes will become leaky modes when bending the fiber.

In this paper, we design a novel fiber with special structure, called the single-trench fiber (STF, produced by Yangtze Optical Fiber and Cable Joint Stock Limited Company), which has two core layers and two cladding layers. On the one hand, it can support more transverse modes with smaller effective refractive index difference between neighboring modes.[22] On the other hand, high-order modes can continue to transport in the second core layer as transmitting modes when bending the fiber. Thus, power distribution among different modes of STF can be modulated effectively through bending, thereby reducing coherence of the output light. Our results show that the speckle contrast of output can be decreased considerably by bending the STF. As a result, speckle contrast of less than 0.1 can be realized using a relatively short segment of the STF, which can also be tuned easily by changing the bending turns. However, compared with the STF, an inverse phenomenon is found when using an MMF, e.g., as the MMF bends, the speckle contrast of output increases. This work provides a convenient and tunable way to control the output coherence,

*Project supported by the National Natural Science Foundation of China (Grant Nos. 11974071 and 61635005) and in part by Sichuan Science and Technology Program, China (Grant No. 2018HH0148).

†Corresponding author. E-mail: wl_zhang@uestc.edu.cn

© 2020 Chinese Physical Society and IOP Publishing Ltd

which is of great importance in applications such as free-space optical telecommunications and speckle-free imaging.

2. Detail of the experiment

Schematic cross-section and refractive index profile of the STF and MMF are shown in Fig. 1, where dark and bright regions represent high ($n_1 = 1.4681$) and low ($n_2 = 1.4420$) refractive indexes, respectively. As can be seen from Fig. 1(a), there is a high-index core and the second core layer separated by a low-index trench. The structure parameters marked in Figs. 1(b) and 1(d) are $d = 104$ μm, $\Delta = 2$ μm, $a = 20$ μm, $b = 26$ μm, $L = 105$ μm and $p = 20$ μm. Figure 1(e) shows the calculated effective refractive index (n_{eff}) of the first 500 transverse modes supported by the two fibers with the help of Mode Solution Software. With an increase of mode order, the modal n_{eff} of the STF decreases more slowly than that of the MMF. This is because the STF has the second core layer (which has a refractive index higher than the trench), which causes n_{eff} of high-order modes increasing. As a result, it is easier to tune the power distribution among different modes of the STF through mode coupling.

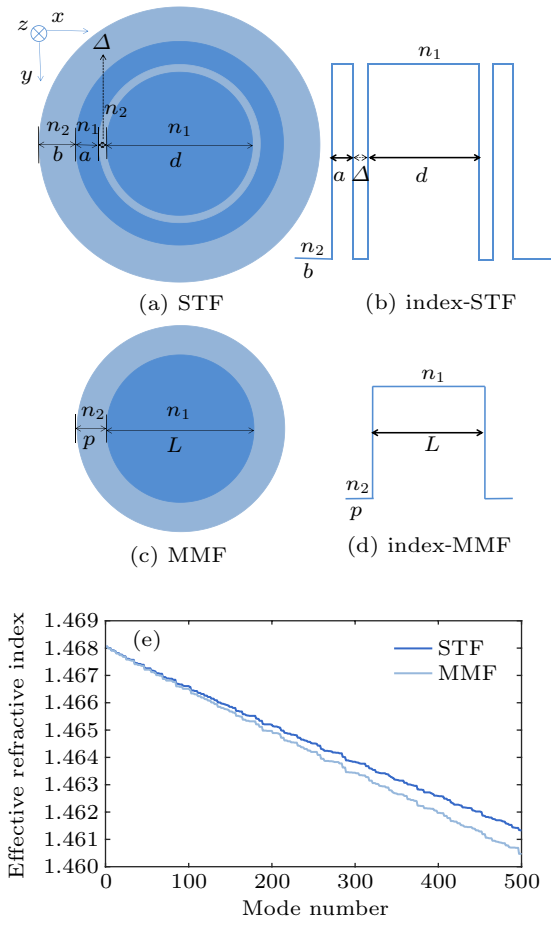


Fig. 1. Characteristics of the two fibers. (a)/(b) and (c)/(d) are schematic cross-section/refractive index profile of the STF and MMF, respectively. (e) Calculated n_{eff} of the first 500 spatial modes. The dark and light line represents the n_{eff} of STF and MMF, respectively.

Some representative field distribution of low-order and high-order modes of the two fibers are shown in Fig. 2. It is observed that, in the STF, the low-order modes distribute mainly in the first core region, and the high-order modes distribute in both the first and second core regions. This is different from the MMF and results in different decoherent procedures when bending the fiber. For example, the leaky modes of the first core may couple into the second core layer when bending the STF, which increases the mode number and is helpful to reduce the spatial coherence.

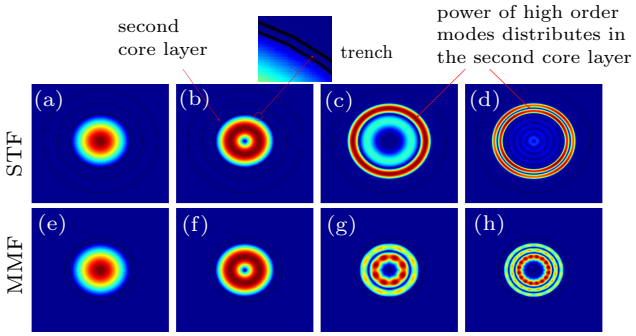


Fig. 2. The power distribution of low-order and high-order modes in the STF and MMF.

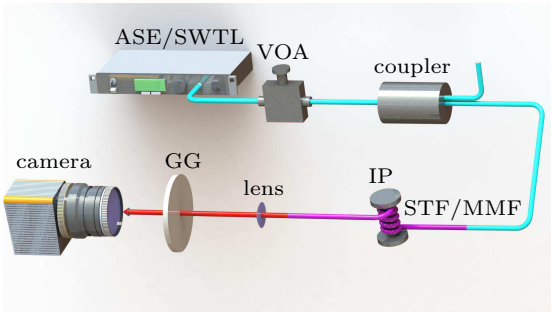


Fig. 3. Schematic diagram of experimental setup. ASE, amplified spontaneous emission. SWTL, swept-wavelength tunable laser. VOA, variable optical attenuator. STF, single trench fiber. MMF, multimode fiber. GG, ground glass.

The experimental setup is schematically shown in Fig. 3. An amplified spontaneous emission (ASE) source with a central wavelength of 1530 nm and bandwidth of ∼7 nm or a swept-wavelength tunable laser (SWTL) light source is launched into a variable optical attenuator (VOA) which is used to control the optical power. A 3 dB coupler, splitting the input light into two beams, is connected with the end of the VOA. One output port of the coupler is followed by a power meter to monitor the optical power and the other port is sliced with a segment of the STF or MMF to reduce the spatial coherence.[23] Speckle patterns are measured by an infrared camera (Xenics, Bobcat-640-GigE) after the light is collimated by a lens (focal length of 6.2 mm) and passing through a ground glass (GG) diffuser. To tune the spatial coherence, the STF and MMF are bent with a bending radius of 1 cm. As for bending loss, we once performed an experiment to study

the change of C when we winded the two fibers. The result shows that the C does not change significantly with the change of bending radius. Thus it is not considered in the following analysis.

3. Study of spatial decoherence

Firstly, output field patterns of the 0.8-m-long STF (Figs. 4(a)–4(e)) or MMF (Figs. 4(f)–4(j)) bent into different turns are recorded using the camera. In the STF, the field distribution extends outwardly and becomes more even with increasing turns of bending, indicating that high-order transverse modes are excited through mode coupling. In the MMF, the field distribution becomes more localized when increasing turns of bending, as the excited high-order modes partially become leaky modes.

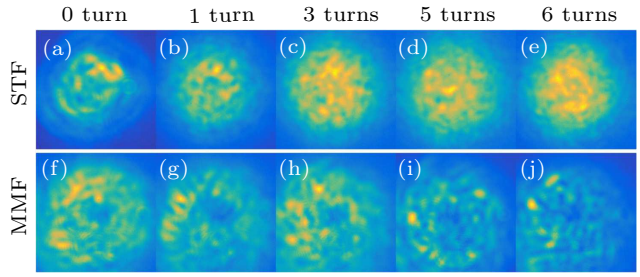


Fig. 4. Mode field profiles of output from the STF (a)–(e) and the MMF (f)–(j) bent 0, 1, 3, 5, 6 turns. The bending radius is 1 cm.

Under the same experimental conditions, the speckle pattern of the output is also measured via inserting a ground glass (GG) before the camera. It can be seen from Figs. 5(a)–5(d) that speckle formation from the output of STF is well prevented and the power distribution becomes more averaged as the number of turns increasing. While the output of the MMF shows an inverse trend, as presented in Figs. 5(e)–5(h), more speckle grains appear with increasing the turns. Linking these speckle patterns with mode field profiles aforementioned in Fig. 4, it is obvious that the more the power profile is averaged, the fewer the speckle grains occur in speckle patterns.

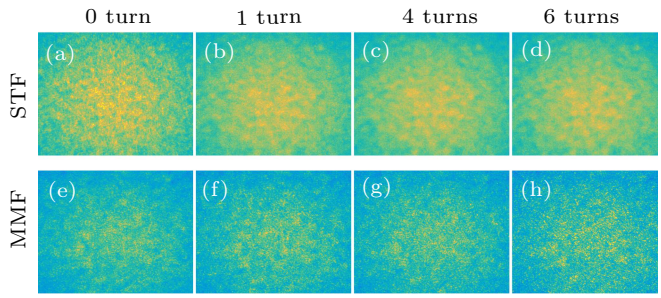


Fig. 5. Speckle patterns formed after light passing through a ground glass diffuser for the STF (a)–(d) and the MMF (e)–(h) bent 0, 1, 4, and 6 turns. The bending radius is 1 cm.

Spatial coherence can be analyzed quantitatively through speckle contrast C of the speckle patterns, which is defined as $C = \sigma_I/\langle I\rangle$ (where σ_I is the standard deviation of the intensity and $\langle I\rangle$ is the average intensity).[24,25] Figure 6 shows the value of C as a function of bending turns N for different lengths of the STF and MMF. When the length is 0.8 m, the blue line marked by circles shows that C of the STF decreases with N, while C of the MMF (the green line with circles) shows an inverse trend. These are in agreement with the results of speckle patterns shown in Fig. 5. The change of speckle contrast is listed in Table 1. In particular, for the first two turns ($N = 2$), C of the STF decreases by around 35% dramatically and keeps almost unchanged (around 0.0855) for further increase of N. While C of the MMF keeps increasing with N, e.g., C increases by 58.6% from $N = 0$ to $N = 6$. When the length is 0.4 m, the result is similar. When the length increases to 3 m, C becomes less than 0.1 and varies little with N for both the STF and MMF. This is due to the fact that intermodal delay surpasses the coherence length of the input light as dispersion increases with transmission length, which is consistent with the theory given in Ref. [20]. We also find that, for the same value of N, the longer the fiber, the smaller the value of C. However, compared with changing the length of the fiber, fiber bending would be more preferred in some applications, since it can modulate the coherence of output more flexibly. Theoretically, the number of spatial modes that effectively[26] affect C can be estimated by $M = C^{-2}/2$, where the denominator 2 refers to polarization mixing in the fibers. Taken $N = 2$ and 0.8-m-long length as an example, the numbers of spatial modes in the STF and MMF are around 30 and 20, respectively.

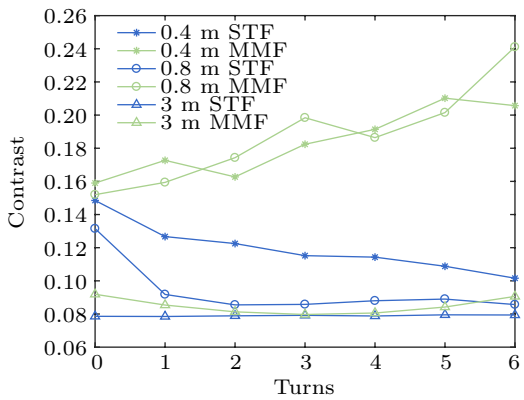


Fig. 6. Speckle contrast of the STF and MMF as a function of the turn. Bending radius is 1 cm. Blue lines and green lines correspond to the STF and MMF, respectively. Here $*$, $\circ$ and $\triangle$ correspond to 0.4 m, 0.8 m and 3 m fibers, respectively. The specific change of C is listed in Table 1.

Table 1. Change of speckle contrast.

Length/m	Minimum C	Maximum C	ΔC
0.4(STF)	0.1016	0.1485	−31.6%
0.8(STF)	0.0855	0.1315	−35.0%
3.0(STF)	0.0786	0.0794	−1.0%
0.4(MMF)	0.1590	0.2102	+32.2%
0.8(MMF)	0.1520	0.2411	+58.6%
3.0(MMF)	0.0797	0.0917	+15.1%

Power distribution among different modes can be further analyzed using the mode decomposition method.[27,28] To get intensity fluctuation of specific regions of the output field as a function of wavelength (i.e., transmission spectrum), the mode profile is recorded continually by the camera when input wavelength is scanned (by the SWTL) from 1520 nm to 1540 nm with 0.5 nm wavelength intervals. Figure 7 gives the transmission spectra of the STF/MMF and the corresponding fast Fourier transform (FFT). The dark-color curve corresponds to $N = 2$, and the light-color curve corresponds to $N = 0$. It is obvious that the transmission spectra of the bent fibers (dark curves) are lower than naturally stretched-out fibers (light curves). The gap between the dark and light curves for the STF is smaller than that for the MMF, which also indicates that the STF has less leaky modes due to the protection of the second core region.

The FFT curves in Figs. 7(b) and 7(d) reflect that components of the transmitted light arrive at the output end with different delays (taking the fundamental mode as a reference). Especially, several peaks appear, corresponding to different orders of mode, and the peaks with larger delay correspond to higher order modes. In Fig. 7(b), we can see that amplitude of high-order modes in the bent fiber is larger than that in the unbent fiber when time delay > 2 ps. This reflects that the power couples from low-order modes to high-order modes and distributes more even when bending the STF. This is in accordance with the conclusion in Ref. [29]. Figure 7(d) reflects that the power of high-order modes decreases due to mode leaking when bending the MMF. All these are in accordance with the conclusion from Figs. 5 and 6.

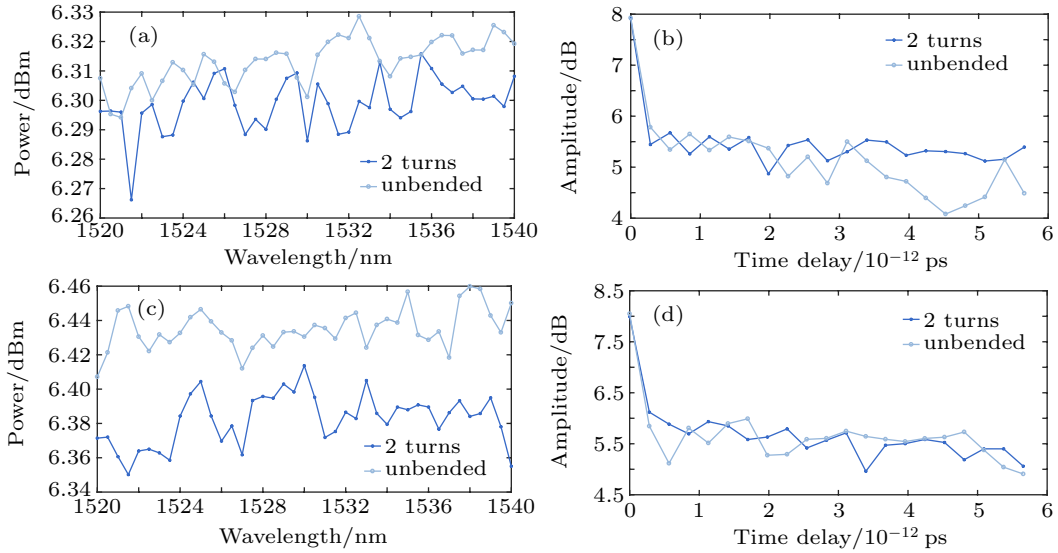


Fig. 7. Transmission spectra of the two fibers and their FFT curves. Bending radius is 1 cm. (a) and (b) Optical spectra of the STF and its FFT result. (c) and (d) Optical spectra of the MMF and its FFT result.

4. Conclusion

In summary, we have proposed an STF and it is used to reduce speckle contrast of fiber light source, the result is also compared with an MMF. It is found that speckle contrast of light sources can be reduced efficiently by bending the STF with only a few meters of length, while the MMF has an inverse influence on the speckle contrast when bending it. Through optical field imaging and decoupling-mode analysis, it is revealed that the inter-mode power distribution in the STF becomes greater even because its second core layer can support high-order modes to transport in it, and this contributes to the reduction of the speckle contrast (i.e., spatial coherence), while high-order modes become leaky modes in the MMF when bending it, and this results in increase of the speckle contrast. The proposed work provides a significant way to analyze/understand modal evaluation in special fibers, as well as to modulate spatial coherence of light source, which are usefully in applications of optical sensing, speckle-free imaging and illuminating.[30]

References

[1] Goodman J W 2007 *Speckle Phenomena in Optics: Theory and Applications* (Englewood, Colorado: Roberts Company) p. 201

[2] Guo G J and Shao Y 2004 *Acta Phys. Sin.* **7** 2089 (in Chinese)

[3] Liang M D, Chen L, Hu Y H, Lin W T and Chen Y H 2018 *Chin. Phys. B* **27** 104202

[4] Wang D Y, Wang Y X, Guo S, Rong L and Zhang Y Z 2014 *Acta Phys. Sin.* **63** 154205 (in Chinese)

[5] Chen Z Y, Li Z G, She W J and Xia A L 2019 *Acta Phys. Sin.* **68** 054206 (in Chinese)

[6] Redding B, Cerjan A, Huang X, Lee M L, Stone A D, Choma M A and Cao H 2015 *Proc. Natl. Acad. Sci. USA* **112** 1304

[7] Fercher A F, Drexler W, Hitzenberger C K and Lasser T 2003 *Rep. Prog. Phys.* **2** 239

[8] Drexler W and Fujimoto J G 2008 *Optical Coherence Tomography: Technology and Applications* (Berlin: Springer) p. 33

[9] Carvalho M T, Lotay A S, Kenny F M, Girkin J M and Gomes A S L 2016 *Proc. SPIE* **9701** 97010Q

[10] Kim J, Miller D T, Kim E K, Oh S, Oh J H and Milner T E 2005 *J. Biomed Opt.* **10** 064034

[11] Desjardins A E, Vakoc B J, Tearney G J and Bouma B E 2006 *Opt. Express* **11** 4736
[12] Szkulmowski M, Gorczynska I, Szlag D, Sylwestrzak M, Kowalczyk A and Wojtkowski M 2012 *Opt. Express* **2** 1337
[13] Liba O, Lew M D, SoRelle E D, Dutta R, Sen D, Moshfeghi D M, Chu S and Zerda A 2017 *Nat. Commun.* **8** 12
[14] Wang F, Liu X L, Yuan Y S and Cai Y J 2013 *Opt. Lett.* **11** 1814
[15] Mehta D S, Naik D N, Singh R K and Takeda M 2012 *Appl. Opt.* **12** 1894
[16] Liu Y L, Yang W H, Xiao S M, Zhang N, Fan Y B, Qu G Y and Song Q H 2019 *ACS Nano* **9** 10653
[17] Efimov A 2014 *Opt. Express* **33** 15577
[18] Manni J G and Goodman J W 2012 *Opt. Express* **10** 11288
[19] Ma R, Zhang W L, Guo J Y and Rao Y J 2018 *Opt. Express* **20** 26758
[20] Ma R, Rao Y J, Zhang W L and Hu B 2019 *IEEE J. Sel. Top. Quantum Electron.* **25** 0900106
[21] Ma R, Li J Q, Guo J Y, Wu H, Zhang H H, Hu B, Rao Y J and Zhang W L 2019 *Opt. Express* **6** 8738
[22] Jain D and Sahu J K 2016 *J. Lightwave Technol.* **14** 3412
[23] Efimov A 2018 *Opt. Lett.* **19** 4767
[24] Redding B, Choma M A and Cao H 2012 *Nat. Photon.* **7** 497
[25] Hokr B H, Schmidt M S, Bixler J N, Dyer P N, Noojin G D, Redding B, Thomas R J, Rockwell B A and Cao H 2016 *J. Mod. Opt.* **1** 46
[26] Redding B, Ahmadi P, Mokan V, Seifert M, Choma M A and Cao H 2015 *Opt. Lett.* **20** 4607
[27] Minh N D, Blin S, Nam N T, Le S D, Provino L, Thual M and Chartier T 2012 *Appl. Opt.* **4** 450
[28] Nicholson J W, Yablon A D, Ramachandran S and Ghalmi S 2008 *Opt. Express* **10** 7233
[29] Ma R, Zhang H H, Egor M, Srikanth S, Wu H, Zhang W L, Vladislav D, Hu T P, Hu Z J, Rao Y J and Sergei K T 2020 *Opt. Express* **14** 20587
[30] Ma R, Wang Z, Zhang H H, Zhang W L and Rao Y J 2020 *Opt. Lett.* **13** 3816